

# Effect of correlations on heat transport in a magnetized strongly coupled plasma

T. Ott,<sup>1</sup> M. Bonitz,<sup>1</sup> and Z. Donkó<sup>2</sup>

<sup>1</sup>Christian-Albrechts-University Kiel, Institute for Theoretical Physics and Astrophysics, Leibnizstraße 15, 24098 Kiel, Germany

<sup>2</sup>Institute for Solid State Physics and Optics, Wigner Research Centre for Physics, Hungarian Academy of Sciences, H-1525 Budapest, P.O.B 49, Hungary

(Received 10 June 2015; revised manuscript received 1 October 2015; published 9 December 2015)

In a classical ideal plasma, a magnetic field is known to reduce the heat conductivity perpendicular to the field, whereas it does not alter the one along the field. Here we show that, in strongly correlated plasmas that are observed at high pressure and/or low temperature, a magnetic field reduces the perpendicular heat transport much less and even *enhances* the parallel transport. These surprising observations are explained by the competition of kinetic, potential, and collisional contributions to the heat conductivity. Our results are based on first-principle molecular dynamics simulations of a one-component plasma.

DOI: 10.1103/PhysRevE.92.063105

PACS number(s): 52.27.Gr, 52.25.Fi, 52.27.Lw

## I. INTRODUCTION

Strongly coupled plasmas have become a focal point of plasma research in recent years as several experimental setups, such as dusty plasmas [1,2], trapped ions [3], and ultracold plasmas [4], have become available to study this unusual state of ionized matter in which the potential energy exceeds the kinetic energy. Similar plasma conditions are thought to exist, e.g., in white dwarf stars or in the outer layers of neutron stars [5,6]. Often, these plasmas are subject to strong magnetic fields, as is the case in neutron stars [7]. Here, a crucial issue is the cooling process [8] that may be strongly influenced by the ionic heat conductivity perpendicular to the field lines [9]. Another example are laser fusion experiments at NIF and Omega where strong ionic coupling occurs during the early compression stage in the cold fuel surrounding the hot spot, and strong self-generated magnetic fields arising from the extreme temperature gradients were observed [10]. Further, in magnetized liner inertial fusion (MagLif) experiments at Sandia [11], very strong magnetic fields are generated, and strong ionic coupling may occur due to highly charged ions and liner mix into the fuel [12]. Finally, the “quasimagnetization” in rotating dusty plasmas represents an experimentally accessible system in which particle-level resolution of strongly coupled, strongly magnetized dust particles is possible [13–15].

For all these systems, the capability of a strongly coupled plasma to conduct and transport or, conversely, to retain heat is crucial. For many applications, such as inertial fusion, an effective thermal insulation of the heated and compressed region plays a key role for the success of the device. Thus, there is a high need for reliable theoretical predictions for the heat conductivity of plasmas that are both strongly coupled and magnetized [16–26].

The interplay between strong particle interaction and a strong magnetic field gives rise to a rich dynamics [16], including complex wave spectra [17–19], generation of higher harmonics [20,21], and long-lived metastable states [22]. The diffusive particle transport has been analyzed in two and three dimensions [23–25] and in binary plasmas [26] with the conclusion that the self-diffusion coefficient is strongly reduced by both the strong coupling and the magnetic field. The viscosity of strongly coupled plasmas has been investigated only for unmagnetized systems [27–29].

Heat transport is well understood in magnetized weakly coupled plasmas since the pioneering work of Braginskii [30] and was studied in strongly coupled unmagnetized systems, e.g., in dusty plasma experiments [31–33], by kinetic theory [34], and by computer simulations [35–40]. However, until now a systematic study of heat transport in *magnetized strongly coupled plasmas* has not been carried out [41]. It is the goal of this work to fill this gap. Since at the moment a self-consistent accurate treatment of all plasma components is not feasible, we concentrate on a one-component plasma (OCP), which is a well-established model for the heavy plasma component in the presence of strong correlations in thermal equilibrium [43–46]. The light component (electrons) enters via the screening length  $\bar{\kappa}^{-1}$  of the ion-ion interaction potential:

$$\phi(r) = Q^2/r \times \exp(-\bar{\kappa}r). \quad (1)$$

The limitations of this Yukawa OCP (YOCP) model and the validity of our results will be discussed below. For the YOCP, it is possible to perform a comprehensive first principles molecular dynamics (MD) analysis. This allows us to show that the heat conductivity  $\lambda$  in strongly coupled plasmas radically differs from that in weakly correlated high-temperature plasmas [30,47]: (a) the reduction of  $\lambda_{\perp}$  (the component perpendicular to  $\mathbf{B}$ ) with increasing magnetic-field strength  $B$  is much slower and  $\lambda_{\perp}$  approaches a nonzero asymptotic value, and (b) the parallel component  $\lambda_{\parallel}$  *increases* with  $B$  instead of remaining constant. An explanation of the physical mechanisms is presented.

## II. THEORY AND SIMULATION APPROACH

In a magnetized system, the energy flux  $\mathbf{j}$  is related to the temperature gradient via the thermal conductivity tensor as

$$j_{\mu} = -\lambda_{\mu\nu}(\nabla T)_{\nu}, \quad (2)$$

where the latter has three independent components (we assume  $\mathbf{B} \parallel \hat{\mathbf{e}}_z$ ):

$$\underline{\underline{\lambda}} = \begin{pmatrix} \lambda_{\perp} & \lambda_{\times} & 0 \\ -\lambda_{\times} & \lambda_{\perp} & 0 \\ 0 & 0 & \lambda_{\parallel} \end{pmatrix}. \quad (3)$$

The components  $\lambda_{\parallel}$  and  $\lambda_{\perp}$  describe field-parallel and cross-field heat transport, respectively, and converge to the scalar heat conductivity  $\lambda = \lambda_0$  as  $B \rightarrow 0$ . The off-diagonal term  $\lambda_x$  is the analog of the Hall effect (the so-called Righi-Leduc effect [48]) and vanishes for  $B \rightarrow 0$ .

A microscopic approach to compute  $\lambda_{\mu\nu}$  is provided by the Irving-Kirkwood expression [46,49] for the heat flux,

$$\mathbf{j} = \sum_{i=1}^N \mathbf{v}_i \left[ \frac{1}{2} m |\mathbf{v}_i|^2 + \frac{1}{2} \sum_{j \neq i}^N \phi(r_{ij}) \right] + \frac{1}{2} \sum_{i=1}^N \sum_{j \neq i}^N (\mathbf{r}_{ij} \cdot \mathbf{v}_i) \mathbf{F}_{ij}, \quad (4)$$

which consists of kinetic, potential, and collision contributions (first, second, and last term, respectively). The Green-Kubo formula [50] then yields the heat conductivity tensor as

$$\lambda_{\mu\nu} = \lim_{\tau \rightarrow \infty} \frac{1}{V k_B T^2} \int_0^\tau \langle j_\mu(t) j_\nu(0) \rangle dt, \quad (5)$$

where the integral is over the heat flux autocorrelation function. According to Eq. (4), each component of  $\lambda_{\mu\nu}$  is the sum of three direct and three cross-correlation terms.

We compute  $\lambda_{\mu\nu}$  for a typical strongly coupled YOCP, and apply a homogeneous magnetic field. The results below are for the value  $\kappa = a\tilde{\kappa} = 2$ , where  $a = [3/(4n\pi)]^{1/3}$  is the Wigner-Seitz radius, and are representative (results for other  $\kappa$  values are shown in Appendix A). The system is completely characterized by three dimensionless parameters:

$$\Gamma = Q^2/(k_B T a), \quad (6)$$

$$\kappa = a\tilde{\kappa}, \quad (7)$$

$$\beta = \omega_c/\omega_p \propto B, \quad (8)$$

i.e., the coupling parameter  $\Gamma$ , the screening parameter  $\kappa$ , and the normalized magnetic-field strength  $\beta$ . Here,  $\omega_p = [4\pi Q^2 n/m]^{1/2}$  is the plasma frequency, and  $\omega_c = qB/(mc)$  is the cyclotron frequency ( $Q$ ,  $T$ , and  $c$  are the charge, temperature, and speed of light, respectively). For later use we also define the dimensionless parameter

$$\alpha = \tau_{\text{col}} \omega_p \quad (9)$$

as the product of the the collision time  $\tau_{\text{col}}$  and the plasma frequency.

We performed extensive MD simulations optimized for strong magnetic fields [51,52], using  $N = 8192$  particles in a cubic box with periodic boundary conditions. Data collection begins after an equilibration period and takes place under microcanonic conditions for a time of  $t\omega_p = 2.5 \times 10^5$ . Since the evaluation of the integral Eq. (5) is limited to a finite time  $\tau$  in practice, its value is determined by averaging Eq. (5) over  $\omega_p \tau \in [1000, 2000]$ . For each data point, 50 separate simulations with different initial conditions are averaged for a total measurement time of  $\omega_p t = 1.25 \times 10^7$ . We report the standard error of the mean of these simulations; unless shown, the error bar for all values is (much) smaller than the symbol size. Data for the heat conductivity are given in units of  $n k_B \omega_p a^2$ .

### III. RESULTS

#### A. Unmagnetized system

We start with an isotropic, unmagnetized system where  $\lambda_{\mu\nu}$  is diagonal. Figure 1 reveals an interesting nonmonotonic dependence of  $\lambda$  on  $\Gamma$ , which is one of the hallmarks of strongly coupled systems.

The present results represent a significant improvement in terms of accuracy over previously available data and facilitate a more detailed analysis. In particular, the decomposition Eq. (4) uncovers the origin of this dependency: The kinetic contribution to  $\lambda$  corresponds to the (material) transport of kinetic energy associated with the movement of a particle between collisions. It falls off, approximately as  $\Gamma^{-3/2}$ , since both the mean free path and the thermal energy per particle decrease with  $\Gamma$  [53]. Likewise, the potential contribution is associated with the material transport of potential energy and increases with  $\Gamma$  as the average potential energy grows. In the region of  $\Gamma = 30 \dots 200$  this growth slows down, since the mean free path decreases with  $\Gamma$ , and the system dynamics transform into caged motion. Finally, the collisional part increases with  $\Gamma$  up to the crystallization point ( $\Gamma_c \approx 420$ ), where heat transport is dominated by phonons [9].

We also compare the present results to those reported earlier by Salin and Caillois [36] and Donkó and Hartmann [37]; see Fig. 2. The simulational results are in good agreement, especially at smaller and higher coupling values. Around the minimum of  $\lambda(\Gamma)$ , there are larger deviations of the order of 20%. Careful analysis suggests that this is due to the better statistics of the present data and the considerably larger integration limit  $\tau$  employed in the present calculations, whereas commonly, the integration is only carried out up to the first zero-crossing of the integrand [36]. At intermediate coupling values close to the minimum heat conductivity, we

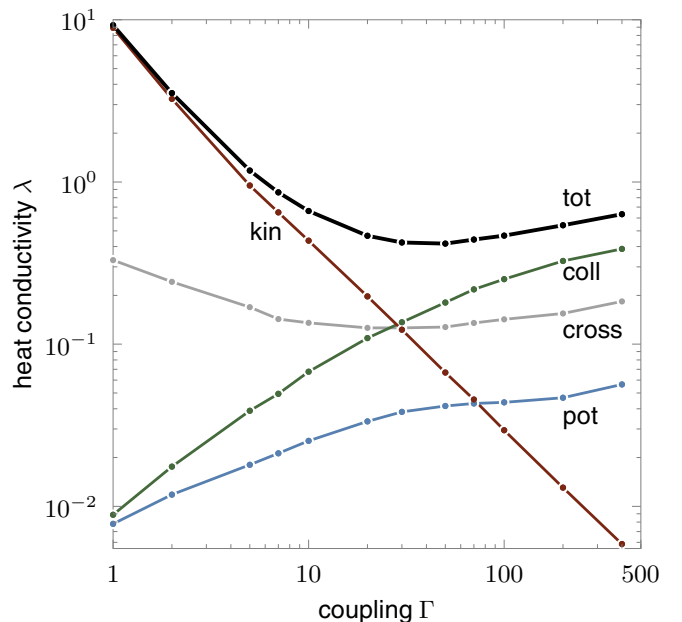


FIG. 1. (Color online) Heat conductivity in an unmagnetized Yukawa system at  $\kappa = 2$  as a function of  $\Gamma$ . Shown are the total conductivity and its kinetic, potential, and collisional parts. “Cross” denotes the sum of the three cross-correlation terms.

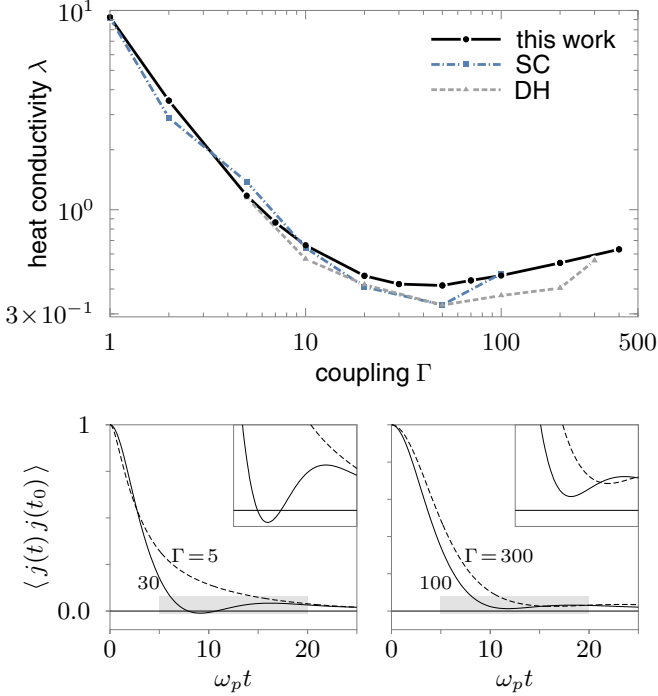


FIG. 2. (Color online) Results for an unmagnetized Yukawa system. Top: Comparison of the heat conductivity results with Salin and Caillol (SC) [36] and Donkó and Hartmann (DH) [37]. Bottom: The (normalized) integrand of Eq. (5) for systems at different values of  $\Gamma$ . The insets show a magnification of the shaded areas.

find that the energy autocorrelation function has an oscillatory time-dependence with negative and positive portions (see bottom part of Fig. 2), which requires a larger integration limit for accurate results.

### B. Cross-field heat transport

In the presence of a magnetic field, the  $\Gamma$ -dependence of  $\lambda$  changes drastically, as is shown in Fig. 3. Consider first the field-perpendicular contribution,  $\lambda_{\perp}$ . As in a weakly coupled plasma,  $\lambda_{\perp}$  is reduced by the magnetic field; however, with increasing  $\Gamma$  this reduction becomes less pronounced. This is readily explained by the change of the governing heat transport mechanisms in different coupling regimes: For small  $\Gamma$ , material transport of kinetic energy dominates (see Fig. 1), which is greatly reduced perpendicular to  $\mathbf{B}$  by the cyclotron motion of the particles. On the other hand, at large  $\Gamma$ , the thermal conductivity is mainly due to collisions between particles (Fig. 1) whose frequency and effectiveness are only weakly reduced by the magnetic field. Figure 4(a) shows how these different effects give rise to the observed  $\Gamma$ -dependence of  $\lambda_{\perp}$  at  $\beta = 1$ .

Let us now analyze the dependence of  $\lambda_{\perp}$  on the magnetic-field strength. For weakly coupled systems, both classical transport theory [30] and a hydrodynamic analysis [54,55] predict a decay of  $\lambda_{\perp}$  scaling as  $\lambda_{\perp} \sim \beta^{-2}$ , whereas the parallel conductivity is independent of the field strength,  $\lambda_{\parallel} \sim \beta^0$ . The corresponding simulation results for strongly correlated systems are shown in Fig. 5 for the cases  $\Gamma = 5$  and  $\Gamma = 40$ .

As observed before,  $\lambda_{\perp}$  decreases with  $\beta$ ; however, it does not vanish, but approaches a finite value. The analysis shows

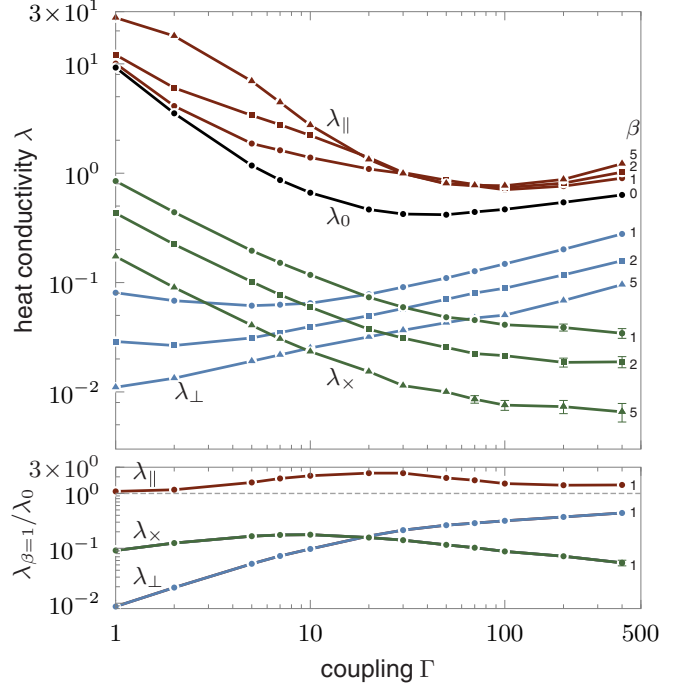


FIG. 3. (Color online) Elements of the heat conductivity tensor at different magnetic-field strengths as a function of  $\Gamma$  (top), and the value at  $\beta = 1$  relative to the field-free value  $\lambda_0$  (bottom).

that this is due to a residual heat transfer via collisions (see Fig. 5): even if particles are unable to move perpendicular to  $\mathbf{B}$ , heat is still transferred by collective modes of the plasma, in particular, the ordinary shear mode and the upper and lower hybrid modes [18], a mechanism similar to heat transfer via phonons in crystals.

### C. Thermal Hall effect

The off-diagonal tensor component  $\lambda_{\times}$  [cf. Figs. 3, 4(b), and 5] is a special case as it emerges only in the magnetic field. However, an increase of  $B$  leads to smaller Larmor radii, which decreases the efficiency of this transport mode. These competing effects result in a nonmonotonic behavior with a maximum around  $\beta = 0.1 \dots 0.5$ , cf. Fig. 5. With increasing coupling  $\lambda_{\times}$  decreases but approaches a finite value, cf. Fig. 4(b), which is explained by the decrease of the Larmor radius with  $\Gamma$  (decrease of temperature) [56].

### D. Field-parallel transport

Figure 3 shows a striking result: heat conduction parallel to  $\mathbf{B}$  is enhanced by the field. This result is surprising, since it is in contrast to the behavior of weakly coupled plasmas. But even for strongly coupled plasmas this is an unexpected field effect as it contradicts the behavior of the diffusion coefficient parallel to  $\mathbf{B}$ , which has been found to decrease monotonically with  $B$  [24]. To clarify the origins of this enhancement, consider again the different contributions to  $\lambda_{\parallel}$ , Fig. 4(c). There is a drastic increase of the collisional contribution compared to the unmagnetized case (Fig. 1), which is easy to understand: collisions parallel to  $\mathbf{B}$  are becoming more effective with increasing field strength, since

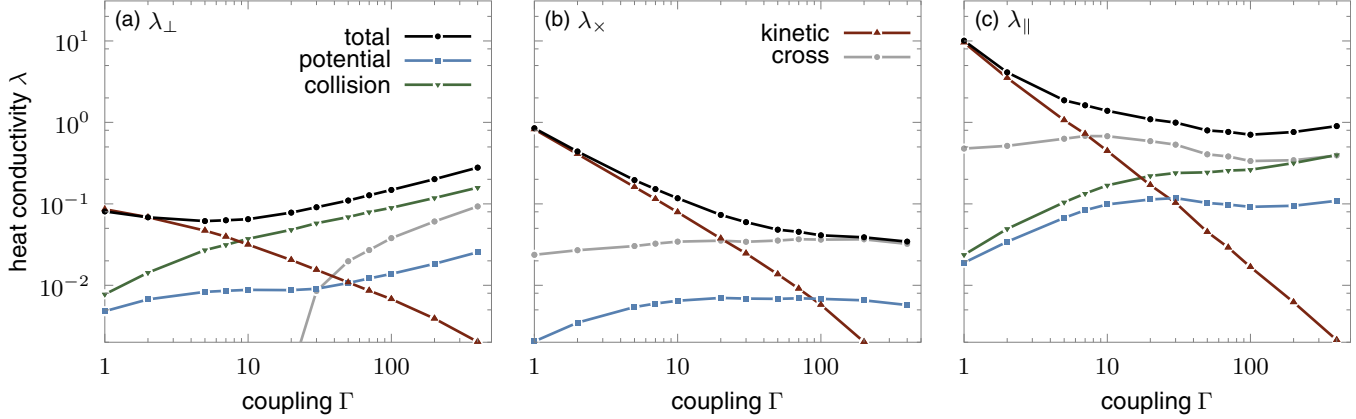


FIG. 4. (Color online) Contributions to the heat conductivities  $\lambda_{\perp}$ ,  $\lambda_x$ , and  $\lambda_{\parallel}$  at  $\beta = 1$ . “Cross” denotes the sum of the three cross-correlation terms.

particles are unable to avoid one another in lateral direction after the initial approach. This leads to a growing interaction time and, subsequently, an increased energy exchange. This is particularly important for moderate coupling ( $\Gamma \lesssim 10$ ), where infrequent binary collisions dominate, and less so in highly coupled systems, where caged motion already results in highly efficient collisions.

The potential contribution to  $\lambda_{\parallel}$  is likewise enhanced by the field. Here, a competition between two processes is observed: On the one hand, the mobility of the particles (i.e., the diffusion coefficient) along  $\mathbf{B}$  is reduced by the field [24]. On the other hand, the reduced interaction with neighboring particles in the cross-field plane enables the particles to retain their

energy for a longer time, resulting in a net increase of the heat conductivity. Similar considerations apply to the kinetic contribution.

The interplay of these processes, together with the varying relative importance of the kinetic, potential, and collisional contributions, work to increase  $\lambda_{\parallel}$  over  $\lambda_0$  for the whole range of coupling strengths considered. Note that the enhancement of  $\lambda_{\parallel}$  is weaker for smaller  $\Gamma$ , and  $\lambda_{\parallel} \rightarrow \lambda_0$  for  $\Gamma \leq 1$  (see Fig. 3), confirming consistency of our simulations with the weak coupling limit. Consider now the dependence  $\lambda_{\parallel}(\beta)$ . As Fig. 5 shows,  $\lambda_{\parallel}$  approaches a maximum value as  $\beta$  increases. This occurs regardless of whether transport is dominated by material transport ( $\Gamma = 5$ ) or by collisions ( $\Gamma = 40$ ). The physical reasons for this is that both the increase of energy retention and of the efficiency of collisions, which are the driving mechanisms behind the growth in  $\lambda_{\parallel}$ , have upper limits, i.e., complete energy retention and complete collisional energy transfer.

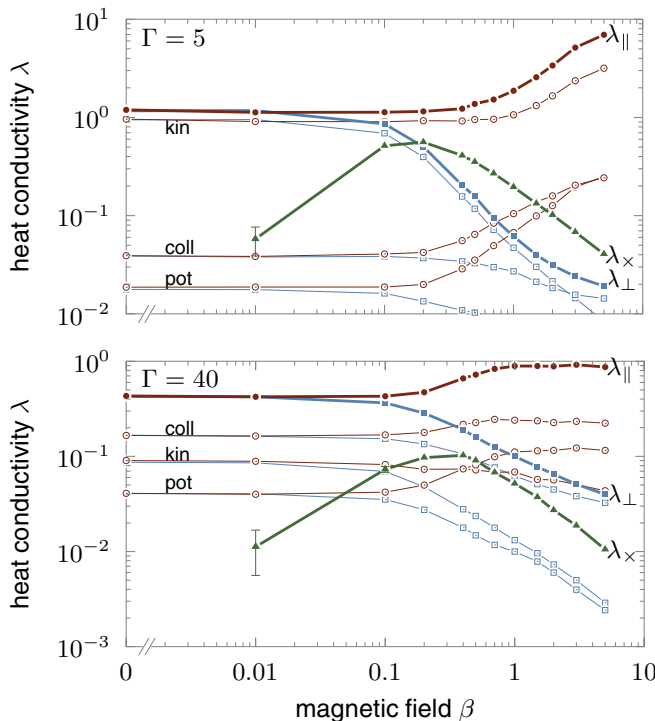


FIG. 5. (Color online) Field dependence of the heat conductivities. Thick lines represent the total values of  $\lambda_{\perp}$ ,  $\lambda_{\parallel}$ , and  $\lambda_x$  and thin lines of the same color and symbol shape show the respective kinetic, potential, and collisional contributions.

### E. Test of classical transport theory

Our simulation results allow us to determine the applicability limits of the weak coupling theory of Braginskii [30,47], which predicts the scalings  $\lambda_{\perp}(\beta) \sim \alpha^{-2}\beta^{-2}$  and  $\lambda_x(\beta) \sim \alpha^{-1}\beta^{-1}$  for large  $\beta$  ( $\alpha = \tau_{\text{col}}\omega_p$  is the normalized collision time). A comparison with the strong coupling data at hand shows semiquantitative agreement for  $\lambda_{\perp}$  and  $\lambda_x$  for moderately coupled plasmas,  $\Gamma \lesssim 5$ , when  $\alpha(\Gamma)$  is regarded as a free parameter. Figure 6 shows the best fit for  $\Gamma = 5$  ( $\alpha = 2.5$ ) and  $\Gamma = 40$  ( $\alpha = 1.24$ ) [57], which indicates excellent (poor) agreement in the former (latter) case. At the same time, this extension of weak coupling theory neither captures the finite asymptotics of  $\lambda_{\perp}$  for large  $\beta$ , nor can it reproduce the increase of  $\lambda_{\parallel}$  with  $\beta$  [59].

### F. Total heat current

Finally, to understand the implications of our results for strongly coupled plasma applications we consider a heated plasma cube of volume  $V$ . The total heat current  $J_T(\Gamma, \beta)$  through the surface (and, thus, the temperature change) will be proportional to [cf. Eq. (3)]  $\lambda^{\text{eff}} = \text{Tr}_{\perp} = \lambda_{\parallel} + 2\lambda_{\perp}$ . At weak coupling,  $J_T$  can be reduced by increasing the magnetic-field strength—a standard tool in many plasma applications—to one

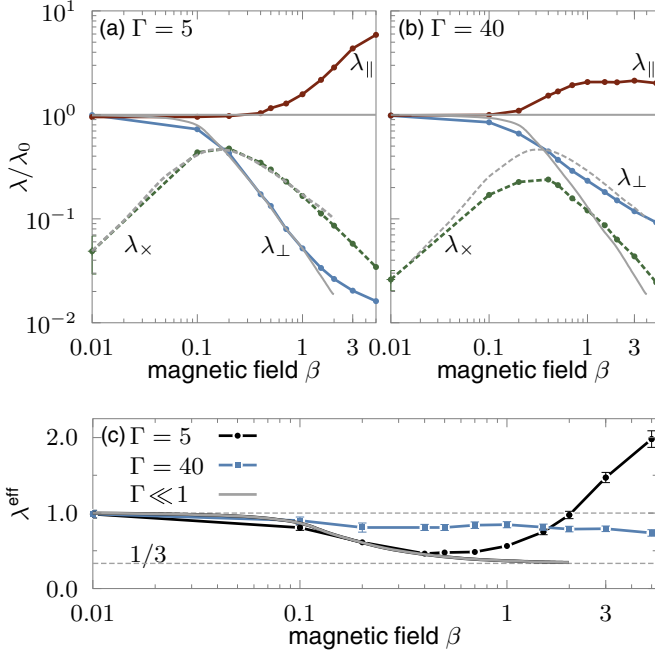


FIG. 6. (Color online) Relative heat conductivities (top) and effective total heat conductivity  $\lambda_{\text{eff}} = \text{Tr}\lambda$  (bottom) compared to classical transport theory for weak coupling, gray curves [47]. To facilitate the comparison, values of  $\alpha = 2.5$  (a, c) and  $\alpha = 1.24$  (b) were used (see text).

third of the field-free value (only  $\lambda_{\parallel}$  remains); see Fig. 6(c). However, in strongly coupled plasmas, our results indicate that using a magnetic field to reduce heat losses is much less effective: for large coupling (cf. curve for  $\Gamma = 40$ ) there is

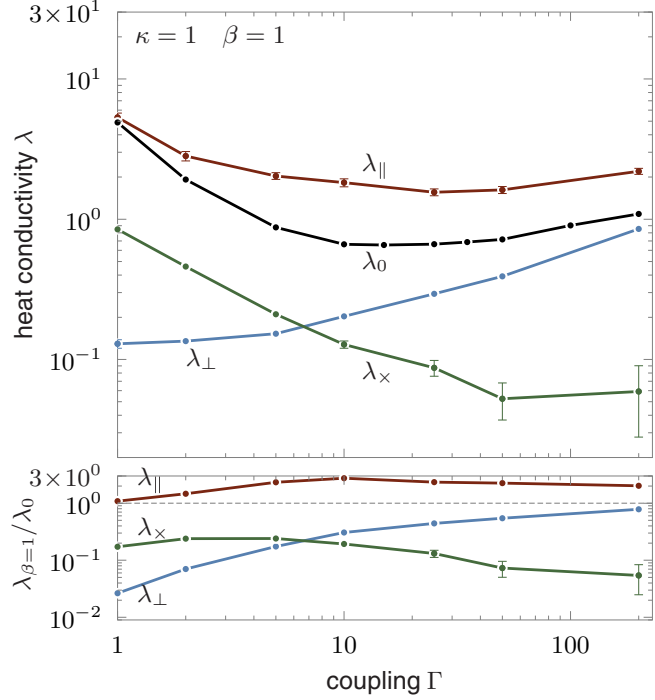


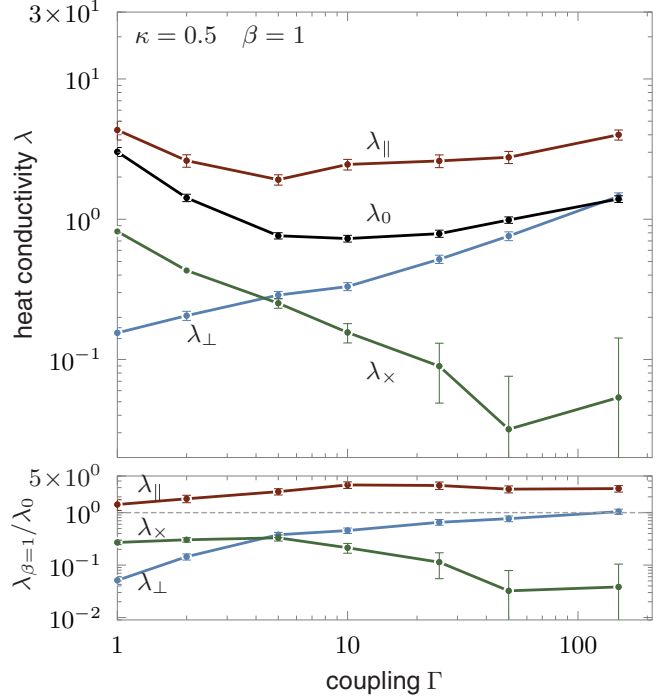
FIG. 7. (Color online) Top: Elements of the heat conductivity tensor for the magnetic-field strength  $\beta = 1$  as a function of  $\Gamma$ . Bottom: Same data relative to the field-free value  $\lambda_0$ . The screening strength is  $\kappa = 1$  (left) and  $\kappa = 0.5$  (right). Compare to Fig. 3 ( $\kappa = 2$ ). Error bars show the standard error of the mean of 240 ( $\kappa = 1$ ) and 50 ( $\kappa = 0.5$ ) shorter simulations and are only shown where larger than the symbol size.

almost no reduction, whereas for moderate coupling (cf. curve  $\Gamma = 5$ ) losses will be reduced for weak fields, but they will be substantially enhanced in strong fields.

#### IV. SUMMARY

We have presented new high-precision data for the thermal conductivity of unmagnetized and magnetized Yukawa one-component plasmas. The decomposition of  $\lambda$  into the different modes of transport (kinetic, potential, and collisional) has enabled us to elucidate the origin of the well-known nonmonotonic dependence of  $\lambda(\Gamma)$  at zero magnetic field for the first time. At finite magnetic fields, the cross-field thermal transport is reduced, as in weakly coupled plasmas; however, the decay is close to  $1/B$  at intermediate field strengths and approaches a finite value at large fields, which is due to the collisional mode. On the other hand and, contrary to what one might expect by extrapolating from the weakly coupled case, the field-parallel heat conductivity is enhanced by the field in strongly coupled plasmas. This is due either to an enhanced energy retention in systems where kinetic transport dominates or due to a modification of the collision process in systems dominated by this transport mode.

Our theoretical predictions can be directly verified in dusty plasmas, using the idea of quasimagnetization in a rotating setup [14,15]. On the other hand, applications to dense plasmas rely on the validity of the OCP model, which is known to be accurate in case of weak electron-ion coupling [43–46]—a reasonable assumption when the electrons are either hot or strongly degenerate. At the same time, the model neglects  $B$ -field effects on the screening [60] as well as the electron contribution  $\lambda^e$  to the heat conductivity. This is justified for



the field-perpendicular component since  $\lambda_{\perp}^i/\lambda_{\perp}^e \sim \sqrt{m_i/m_e}$ , at not too strong coupling [30], as is the case, e.g., in inertial fusion applications. Thus, our results are directly applicable to magnetized plasmas in which the perpendicular heat transport dominates. This includes neutron stars and magnetars with a toroidal field geometry [9] and inertial confinement setups with elongated targets. In particular, for MagLIF our results indicate that the heat insulation of the hot spot may be substantially worse than computed from Braginskii's theory. At the same time these experiments may benefit from increased longitudinal heat conduction, compared to the weakly coupled case [61], as this helps to remove ion density and temperature gradients from the laser preheat stage [12].

### ACKNOWLEDGMENTS

We gratefully acknowledge valuable comments from S. Hansen (Sandia) and A. Potekhin (Ioffe Institute, St. Petersburg). This work is supported by the Deutsche Forschungsgemeinschaft via SFB-TR 24 Project A7, Grant No. shp00006, at the North-German Supercomputing Alliance (HLRN), and Grant No. OTKA-K-105476.

### APPENDIX A: ROLE OF THE SCREENING STRENGTH $\kappa$

In this Appendix, we investigate the role of the screening strength  $\kappa$  for the heat conductivity in a magnetized YOCP. It is well known that, in the unmagnetized case, the heat conductivity  $\lambda$  does not change qualitatively in the range  $\kappa = 0 \dots 2$  [35,37], although the quantitative behavior will be different. As Fig. 7 shows, this also holds in the magnetized case. Particularly, all three components of the heat conductivity tensor depend in the same qualitative way on the coupling strength and the relative change from the unmagnetized case is comparable across all values of  $\kappa$  considered.

### APPENDIX B: ROLE OF MAGNETIC-FIELD NORMALIZATION

Here, we investigate how the choice of the normalization changes the magnetic-field dependence. There are three main

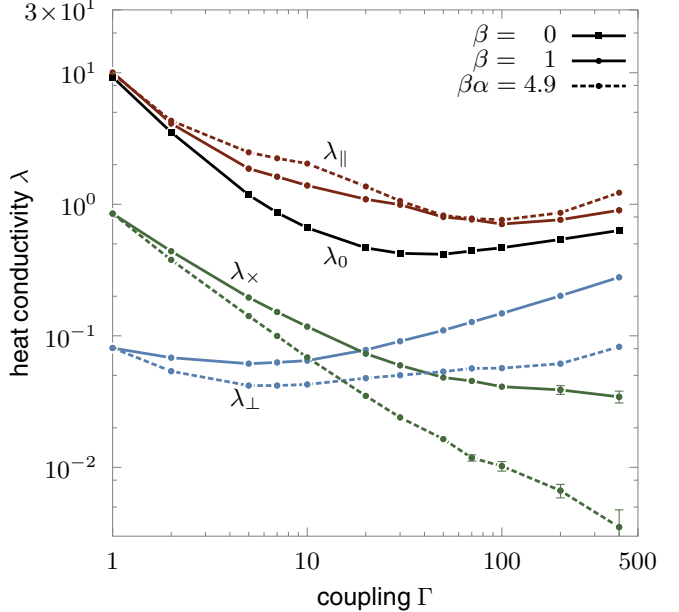


FIG. 8. (Color online) Elements of the heat conductivity tensor for a screening length of  $\kappa = 2$  at different coupling strengths  $\Gamma$ . Shown are the unmagnetized case ( $\lambda_0$ ) and the magnetized system at constant value of  $\beta = \omega_c/\omega_p = 1$  (full lines) and at constant value of  $\beta\alpha = \omega_c\tau_{\text{col}} = 4.9$  (broken lines). For the latter, one has  $\beta\alpha = \sqrt{3\pi/2} \times \Gamma^{-3/2}/\ln \Lambda$  with the effective Coulomb logarithm  $\ln \Lambda$  proposed in Ref. [58].

frequencies in the system—the cyclotron frequency  $\omega_c$ , the plasma frequency  $\omega_p$ , and the collision frequency  $\nu_{\text{col}} = 1/\tau_{\text{col}}$ , corresponding to two dimensionless ratios  $\beta = \omega_c/\omega_p$  and  $\alpha = \omega_p/\nu_{\text{col}}$ . In a strongly coupled plasma,  $\beta$  is used to describe magnetic-field strengths. According to Braginskii [30], however, in a weakly coupled plasma, the magnetic-field effect is captured by a single parameter  $\omega_c/\nu_{\text{col}} = \beta\alpha$ . To test the influence of this choice, we performed additional simulations at fixed  $\beta\alpha$ ; see Fig. 8. Clearly, although the quantitative results differ, the qualitative behavior and trends are not sensitive to the choice of normalization.

- 
- [1] A. Ivlev, G. Morfill, H. Löwen, and C. P. Royall, *Complex Plasmas and Colloidal Dispersions: Particle-resolved Studies of Classical Liquids and Solids*, Series in Soft Condensed Matter (World Scientific Publishing Company, Singapore, 2012).
  - [2] M. Bonitz, C. Henning, and D. Block, Complex plasmas: A laboratory for strong correlations, *Rep. Prog. Phys.* **73**, 066501 (2010).
  - [3] M. J. Jensen, T. Hasegawa, J. J. Bollinger, and D. H. E. Dubin, Rapid Heating of a Strongly Coupled Plasma Near the Solid-Liquid Phase Transition, *Phys. Rev. Lett.* **94**, 025001 (2005).
  - [4] T. C. Killian, T. Pattard, T. Pohl, and J. M. Rost, Ultracold neutral plasmas, *Phys. Rep.* **449**, 77 (2007).
  - [5] S. L. Shapiro and S. A. Teukolsky, *Black Holes, White Dwarfs, and Neutron Stars: The Physics of Compact Objects* (Wiley, New York, 1983).
  - [6] A. Y. Potekhin, The physics of neutron stars, *Phys. Usp.* **53**, 1235 (2010).
  - [7] D. Page, U. Geppert, and M. Küker, Cooling of neutron stars with strong toroidal magnetic fields, *Astrophys. Space Sci.* **308**, 403 (2007).
  - [8] C. J. Pethick, Cooling of neutron stars, *Rev. Mod. Phys.* **64**, 1133 (1992).
  - [9] A. I. Chugunov and P. Haensel, Thermal conductivity of ions in a neutron star envelope, *Mon. Not. R. Astron. Soc.* **381**, 1143 (2007).
  - [10] J. R. Rygg, F. H. Séguin, C. K. Li, J. A. Frenje, M. J.-E. Manuel, R. D. Petrasso, R. Betti, J. A. Delettrez, O. V. Gotchev, J. P. Knauer, D. D. Meyerhofer, F. J. Marshall, C. Stoeckl, and W. Theobald, Proton radiography of inertial fusion implosions, *Science* **319**, 1223 (2008).

- [11] M. R. Gomez *et al.*, Experimental Demonstration of Fusion-Relevant Conditions in Magnetized Liner Inertial Fusion, *Phys. Rev. Lett.* **113**, 155003 (2014).
- [12] S. Hansen, private communication (2015).
- [13] H. Kähler, J. Carstensen, M. Bonitz, H. Löwen, F. Greiner, and A. Piel, Magnetizing a Complex Plasma Without a Magnetic Field, *Phys. Rev. Lett.* **109**, 155003 (2012).
- [14] P. Hartmann, Z. Donkó, T. Ott, H. Kähler, and M. Bonitz, Magnetoplasmons in Rotating Dusty Plasmas, *Phys. Rev. Lett.* **111**, 155002 (2013).
- [15] M. Bonitz, H. Kähler, T. Ott, and H. Löwen, Magnetized strongly coupled plasmas and how to realize them in a dusty plasma setup, *Plasma Sources Sci. Technol.* **22**, 015007 (2013).
- [16] K. N. Dzhumagulova, R. U. Masheeva, T. S. Ramazanov, and Z. Donkó, Effect of magnetic field on the velocity autocorrelation and the caging of particles in two-dimensional Yukawa liquids, *Phys. Rev. E* **89**, 033104 (2014).
- [17] T. Ott, D. A. Baiko, H. Kähler, and M. Bonitz, Wave spectra of a strongly coupled magnetized one-component plasma: Quasilocalized charge approximation versus harmonic lattice theory and molecular dynamics, *Phys. Rev. E* **87**, 043102 (2013).
- [18] T. Ott, H. Kähler, A. Reynolds, and M. Bonitz, Oscillation Spectrum of a Magnetized Strongly Coupled One-Component Plasma, *Phys. Rev. Lett.* **108**, 255002 (2012).
- [19] L.-J. Hou, Z. L. Mišković, A. Piel, and M. S. Murillo, Wave spectra of two-dimensional dusty plasma solids and liquids, *Phys. Rev. E* **79**, 046412 (2009).
- [20] M. Bonitz, Z. Donkó, T. Ott, H. Kähler, and P. Hartmann, Nonlinear Magnetoplasmons in Strongly Coupled Yukawa Plasmas, *Phys. Rev. Lett.* **105**, 055002 (2010).
- [21] T. Ott, M. Bonitz, P. Hartmann, and Z. Donkó, Higher harmonics of the magnetoplasmon in strongly coupled Coulomb and Yukawa systems, *Phys. Rev. E* **83**, 046403 (2011).
- [22] T. Ott, H. Löwen, and M. Bonitz, Magnetic Field Blocks Two-Dimensional Crystallization in Strongly Coupled Plasmas, *Phys. Rev. Lett.* **111**, 065001 (2013).
- [23] B. Bernu, One-Component Plasma in a Strong Uniform Magnetic Field, *J. Phys. Lett.* **42**, 253 (1981).
- [24] T. Ott and M. Bonitz, Diffusion in a Strongly Coupled Magnetized Plasma, *Phys. Rev. Lett.* **107**, 135003 (2011).
- [25] Y. Feng, J. Goree, B. Liu, T. P. Intrator, and M. S. Murillo, Superdiffusion of two-dimensional Yukawa liquids due to a perpendicular magnetic field, *Phys. Rev. E* **90**, 013105 (2014).
- [26] T. Ott, H. Löwen, and M. Bonitz, Dynamics of two-dimensional one-component and binary Yukawa systems in a magnetic field, *Phys. Rev. E* **89**, 013105 (2014).
- [27] Z. Donkó and P. Hartmann, Shear viscosity of strongly coupled Yukawa liquids, *Phys. Rev. E* **78**, 026408 (2008).
- [28] J. Daligault, Liquid-State Properties of a One-Component Plasma, *Phys. Rev. Lett.* **96**, 065003 (2006).
- [29] Z. Donkó, J. Goree, and P. Hartmann, Complex viscosity of 3d Yukawa liquids, *AIP Conf. Proc.* **1397**, 307 (2011).
- [30] S. I. Braginskii, *Transport Processes in a Plasma*, edited by M. A. Leontovich, Reviews of Plasma Physics, Vol. 1 (Consultants Bureau, New York, 1965).
- [31] S. Nunomura, D. Samsonov, S. Zhdanov, and G. Morfill, Heat Transfer in a Two-Dimensional Crystalline Complex (dusty) Plasma, *Phys. Rev. Lett.* **95**, 025003 (2005).
- [32] V. E. Fortov, O. S. Vaulina, O. F. Petrov, M. N. Vasiliev, A. V. Gavrikov, I. A. Shakova, N. A. Vorona, Yu. V. Khrustalyov, A. A. Manohin, and A. V. Chernyshev, Experimental study of the heat transport processes in dusty plasma fluid, *Phys. Rev. E* **75**, 026403 (2007).
- [33] V. Nosenko, S. Zhdanov, A. V. Ivlev, G. Morfill, J. Goree, and A. Piel, Heat Transport in a Two-Dimensional Complex (dusty) Plasma at Melting Conditions, *Phys. Rev. Lett.* **100**, 025003 (2008).
- [34] L. G. Suttorp and J. S. Cohen, Kinetic theory of the collective modes for a dense one-component plasma in a magnetic field, *Physica A* **133**, 370 (1985).
- [35] Z. Donkó and B. Nyíri, Molecular dynamics calculation of the thermal conductivity and shear viscosity of the classical one-component plasma, *Phys. Plasmas* **7**, 45 (2000).
- [36] G. Salin and J.-M. Caillol, Transport Coefficients of the Yukawa One-Component Plasma, *Phys. Rev. Lett.* **88**, 065002 (2002).
- [37] Z. Donkó and P. Hartmann, Thermal conductivity of strongly coupled Yukawa liquids, *Phys. Rev. E* **69**, 016405 (2004).
- [38] Z. Donkó, J. Goree, P. Hartmann, and Bin Liu, Time-correlation functions and transport coefficients of two-dimensional Yukawa liquids, *Phys. Rev. E* **79**, 026401 (2009).
- [39] Yu. V. Khrustalyov and O. S. Vaulina, Numerical simulations of thermal conductivity in dissipative two-dimensional Yukawa systems, *Phys. Rev. E* **85**, 046405 (2012).
- [40] G. Kudelis, H. Thomsen, and M. Bonitz, Heat transport in confined strongly coupled two-dimensional dust clusters, *Phys. Plasmas* **20**, 073701 (2013).
- [41] A preliminary investigation of the effect of a magnetic field on heat transport in a charged two-component system is found in Ref. [42].
- [42] F. Mouhat, S. Bonella, and C. Pierleoni, Charge transport simulations of NaCl in an external magnetic field: The quest for the hall effect, *Mol. Phys.* **111**, 3651 (2013).
- [43] W. D. Kraeft, D. Kremp, W. Ebeling, and G. Röpke, *Quantum Statistics of Charged Particle Systems* (Springer, Berlin, 1986).
- [44] V. E. Fortov, I. T. Iakubov, and H. A. Bronstein, *The Physics of Nonideal Plasma* (World Scientific, New York, 2000).
- [45] S. Ichimaru, *Statistical Plasma Physics* (Westview, New York, 2004).
- [46] J. P. Hansen and I. R. McDonald, *Theory of Simple Liquids* (Academic Press, London, 2006).
- [47] R. Balescu, *Transport Processes in Plasmas, Vol. I: Classical Transport* (North-Holland Publishing Company, Amsterdam, 1988).
- [48] R. T. Delves, Thermomagnetic effects in semiconductors and semimetals, *Rep. Prog. Phys.* **28**, 249 (1965).
- [49] J. H. Irving and J. G. Kirkwood, The statistical mechanical theory of transport processes. iv. The equations of hydrodynamics, *J. Chem. Phys.* **18**, 817 (1950).
- [50] D. J. Evans and G. P. Morriss, *Statistical Mechanics of Nonequilibrium Liquids* (Academic Press, London, 1990).
- [51] Q. Spreiter and M. Walter, Classical molecular dynamics simulation with the velocity verlet algorithm at strong external magnetic fields, *J. Comput. Phys.* **152**, 102 (1999).
- [52] S. A. Chin, Symplectic and energy-conserving algorithms for solving magnetic field trajectories, *Phys. Rev. E* **77**, 066401 (2008).

- [53] Note that for weakly coupled plasmas ( $\Gamma \ll 1$ ),  $\lambda$  is proportional to the product of the mean free path and the thermal velocity, i.e.,  $\lambda_{wc} \propto \Gamma^{-5/2}$  [30].
- [54] M. C. Marchetti, T. R. Kirkpatrick, and J. R. Dorfman, Hydrodynamic theory of electron transport in a strong magnetic field, *J. Stat. Phys.* **46**, 679 (1987).
- [55] M. C. Marchetti, T. R. Kirkpatrick, and J. R. Dorfman, Errata: Hydrodynamic theory of electron transport in a strong magnetic field, *J. Stat. Phys.* **49**, 871 (1987).
- [56] We also note that the collisional contribution to  $\lambda_x$  is zero since only the trajectories of the particles are modified by the magnetic field, but not their interactions.
- [57] The ratio of these values is compatible with the effective Coulomb logarithms for correlated plasmas proposed in Ref. [58].
- [58] S. A. Khrapak, Effective Coulomb logarithm for one component plasma, *Phys. Plasmas* **20**, 054501 (2013).
- [59] The scaling of  $\lambda$  with  $\alpha\beta$  is explored in Appendix B.
- [60] J.-P. Joost, P. Ludwig, H. Kähler, C. Arran, and M. Bonitz, Screened coulomb potential in a flowing magnetized plasma, *Plasma Phys. Controlled Fusion* **57**, 025004 (2015).
- [61] This contribution adds to the dominant electronic contribution where  $\lambda_{\parallel}^e/\lambda_{\parallel}^i \sim \sqrt{m_i/m_e}$ , for  $\Gamma \lesssim 1$  [30].